2016-01-1409
Published 04/05/2016

doi:10.4271/2016-01-1409
saepcmech.saejournals.org

Condensation Modeling during Automotive Lighting Product Development Using CFD Simulation

J. Christopher Watson, Gennady Dumnov, Alexander Muslaev,
Andrey Ivanov, and Svetlana Shtilkind
Mentor Graphics Corp.

ABSTRACT

Condensation occurrence in automotive headlights can be detrimental to consumer acceptance of a product. This paper describes a technique for transient numerical simulation of liquid film formation on surfaces during lighting thermal analysis performed using Computational Fluid Dynamics (CFD), including how the film's properties influence the thermal solution. The numerical technique presented accounts for the change in the film thermal state and thickness due to heat exchange with external fluid flow and solid bodies, surface evaporation/condensation, melting/crystallization within the film volume, and its motion due to gravity and friction forces from the surrounding airflow. Additionally, accurate modeling of radiation effects is critical for lighting applications, including the attendant influence on the thermal distribution of the solids that may have surfaces subject to condensation. Headlights feature large numbers of reflective surfaces and refractive bodies focusing light on local regions and many of the semitransparent materials have absorption coefficients with distinct spectral dependencies. To simulate the thermal loads adequately, the optical behavior of these elements within the system should be modeled accurately as it potentially impacts the formation of the liquid film on the headlight's components. Radiative heat transfer is often calculated with a "band" Monte-Carlo radiation model where the entire spectral range is split into several spectral bands with material properties and boundary conditions averaged within each band. The CFD simulation study presented utilizes an enhanced Monte Carlo Radiation Model which does not require splitting into bands but allows a continuous, accurate representation of spectral material properties, radiation sources and boundary conditions.

CITATION: Watson, J., Dumnov, G., Muslaev, A., Ivanov, A. et al., "Condensation Modeling during Automotive Lighting Product Development Using CFD Simulation," *SAE Int. J. Passeng. Cars - Mech. Syst.* 9(2):2016, doi:10.4271/2016-01-1409.

INTRODUCTION

In observing evaporation or vapor condensation on the surface of solid bodies the formation and subsequent removal of a liquid film is implied. Heat release or absorption is also observed as a phase change takes place. Furthermore, the heat exchange between the solid body and the external gas flow is affected with the liquid film acting like a thermal resistance.

It is desirable for applications such as automotive lighting design to perform computational simulations of this phenomena. Numerical methods have used approaches modeling a liquid film formation by using a dense computational mesh, where the liquid film along its thickness is sufficiently resolved by the cells. However, this requires large computational resources because of the relatively small scales of the film compared to the solid object considered.

This paper details an engineering approach using mathematical models, with stated assumptions, to adequately capture all the essential physical processes while requiring relatively low computational resources for accurate prediction. This is so that analytical design performance studies with computational fluid dynamics (CFD) software are more comprehensive. The modeling approach detailed in this paper is implemented in FloEFD software (Mentor Graphics Corporation). Through 2 validation cases, experimental study results are compared to simulation results for agreement.

This paper then describes a report on the results from a numerical thermal CFD simulation study of a vehicle headlight with complex housing geometry. The aim of the study being to predict the formation of liquid film on the internal surface of a headlight's protective lens with the subsequent removal during operation.

SURFACE CONDENSATION AND FILM FORMATION MATHEMATICAL MODELING

This section details derivation of equations for the simulation of film formation on a surface of a solid body. The thermal state of liquid film and its thickness are influenced by several of the following factors: heat exchange with the outer fluid flow and the solid body; film surface condensation/evaporation; melting/crystallization within the film volume; the film motion caused by gravitation and also due to friction forces from the outer flow.

Below are a list of 9 assumptions necessary of the mathematical modeling approach described:

1. The outer flow fluid is considered a gas mixture with nonzero humidity;
2. Mass transport is diffusive between film and vapor in the outer flow;
3. Equations describing outer fluid flow exclude film thickness, although finite;
4. The derivatives of all primary flow parameters along the normal to the body surface are infinitely large comparing to the ones along the surface;
5. Forces due to inertia within the film are negligibly small compared to viscous and mass forces;
6. Surface tension force is neglected;
7. Film motion is laminar, if present;
8. The film along its thickness is uniform and is either in a liquid or solid state, no sub-layers are considered;
9. The temperature profile is linear along the film thickness.

Equations describing the transport of mass per unit surface and enthalpy can be derived:

$$\frac{\partial m}{\partial t} + \nabla_S m\vec{U} + q_Y = 0 \tag{1}$$

$$\frac{\partial m\overline{h}}{\partial t} + \nabla_S m\vec{U}\overline{h} + q_Y h_v + q_T + q_s = 0 \tag{2}$$

Variable Definitions:

∇_S - surface divergence operator

m - film mass per unit surface

$\overline{h}$ - specific enthalpy of film averaged over its thickness

$\vec{U}$ - film velocity vector

q_Y - mass flux to the gaseous phase (due evaporation or condensation)

h_v - specific enthalpy of vapor in the outer flow calculated at the temperature of film's external surface;

q_T - heat flux to the gaseous phase, q_s - solid surface heat flux;

A vector equation for film velocity averaged over its thickness is derived in the following form given assumptions 4-6:

$$\vec{U} = \frac{\rho_l \delta^2}{3\mu_l} \cdot \vec{g} + \frac{\delta}{2\mu_l} \cdot \vec{\tau}_f \tag{3}$$

Where:

ρ_l, μ_l - density and dynamic viscosity of liquid film material

$\vec{g}$ - gravity force vector projected on the surface

δ - film thickness

$\vec{\tau}_f$ - stress vector on the film's surface.

The equations (1)…(3) are coupled with the equations describing the transport of mass, momentum and energy in the outer flow as well as the equation describing heat conduction in the solid body to form a closed system of equations that is fully implemented in the CFD software.

MONTE-CARLO RADIATION MODELING ACCOUNTING FOR SPECTRAL PROPERTIES - A MODIFIED APPROACH

Accurate radiation heat transfer modeling within a luminaire such as an automotive headlight is a complex analytical challenge. The following points below further highlight radiation modeling complexity for an automotive headlight application with halogen bulb:

- A Tungsten spiral of a halogen bulb may have a temperature in the region of 3000K as the radiation source
- Spectral radiation produced by the spiral interacts with semitransparent and opaque headlight elements.
- The bulb's envelope and the gas within it are heated.
- A heated bulb radiates in the IR spectrum.
- A certain fraction of radiative energy produced by the spiral is absorbed by the envelope material, thus the resulting radiation spectrum and polar pattern.

Given the above physical behavior, it is advantageous for heat transfer simulation accuracy overall to account for the absorbed and radiated heat in the IR spectrum comprehensively.

Simulating spectral effects via classic approaches depends on discretization of the entire spectral range into several bands that each have material properties (absorption coefficient, emissivity) and boundary conditions averaged within each band. There are some complexities that arise at the stage when specifying the band ranges as it is important to ensure that the all the materials properties considered within a certain band vary moderately with the change of wavelength. When many materials have to be specified, such as during industrial design of a product, this type of task becomes very detailed as the number of spectral bands becomes large.

The modified Monte-Carlo radiation model presented, and implemented in the CFD software (FloEFD), does not require splitting into bands. In contrast to "classic" Monte-Carlo model where its direct simulation of a "photon" involves having a certain energy assigned at the "photon" inception time, this modified modeling approach considers "photons" having both the energy and the wavelength assigned at the time of inception. The interaction of a "photon" with the surrounding medium is simulated such that the medium properties and the spectral boundary conditions at certain wavelengths affect only the "photons" of matching wavelength. This means that no averaging of medium properties within a spectral band is performed and instead the "real" properties of the radiating objects are used.

To implement this method there are challenges in obtaining accurate spectral distribution of "photons". This is because distribution depends on the temperature of the radiating objects as well as their emissivity. The latter is dependent on temperature and wavelength so complex spectral functions have to be integrated.

VALIDATION OF LIQUID FILM MODELING APPROACH VS PUBLISHED EXPERIMENTAL STUDIES

This section describes 2 separate comparisons of experimental data to the numerical simulation of surface condensation and liquid film formation performed in the analytical CFD software.

Surface Evaporation in a Rectangular Duct

Film condensation or evaporation of water in a horizontal rectangular duct was analyzed. The experimental study and results are detailed in Iskra and Simpson (2007) [1].

For the numerical analysis the convective mass transfer coefficient between air flowing in the duct and a pan of water is estimated. A pan of water forms the bottom surface of the duct. The considered duct is part of a transient moisture transfer (TFT) facility, shown in Figure 1.

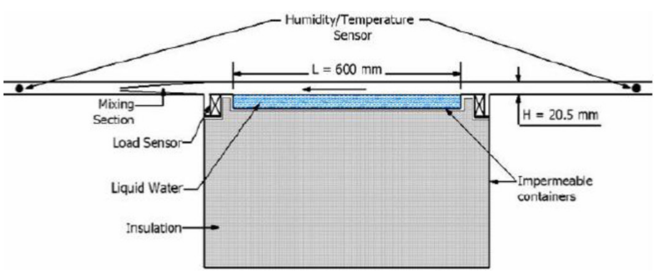

Figure 1. Schematics of the test facility showing a side view of test section (according to Iskra and Simpson (2007).

Conditions and flow regime assumptions for simulation:

- Water temperature = 12°C.
- Air upstream of the test section is 23°C.
- Laminar (R_{eD}=1500) and turbulent (R_{eD}=6000) flow regimes are considered.
- Air relative humidity is 16.2 % for the laminar flow case and 22.9 % for the turbulent flow case 2D and 3D computational domains were considered.
- For the water surface simulation, a condensed water film initial film thickness of 50 μm was set at the bottom of the pan.

Figure 2 shows the transient development of the predicted evaporation rate compared to the experimental data [1]:

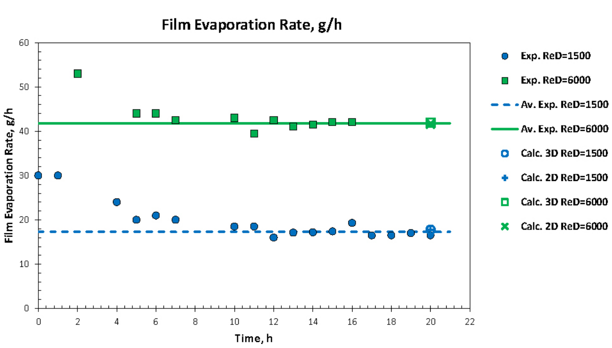

Figure 2. Evaporation rate of water predicted by FloEFD and measured experimentally.

A comparison of the evaporation rates shows there is good agreement between the described CFD numerical method and test results for accuracy. For 2D and 3D calculations, the relative calculation errors do not exceed 1.0% for R_{eD}=6000 and 3.5% for R_{eD}=1500, respectively.

Horizontal Plate - Film-Wise Condensation Simulation

The film condensation process on a cooled surface resulting from the condensation of water vapor from humid air is considered for a horizontal flat plate (area 25 cm^2). The results of the experimental study are given in Tiwari (2011) [2] are compared to numerical calculations using CFD software. The compared test results are from condensation progression under controlled air flow conditions.

Experimental Study summary (based on Tiwari (2011) :

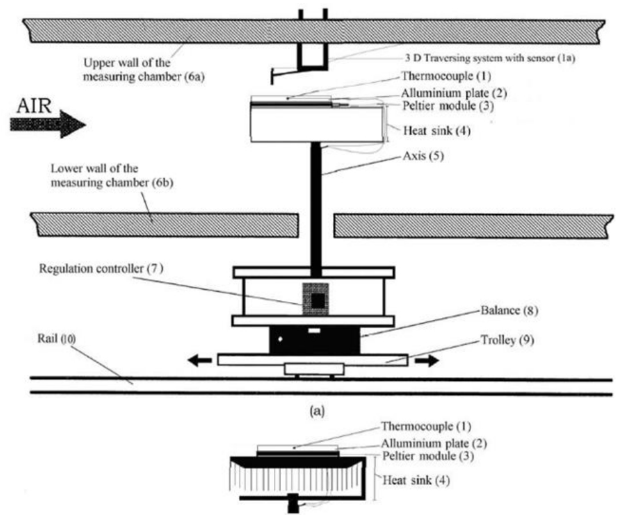

Figure 3. Schematics of the condensation unit (according to Tiwari (2011): (a) front view, (b) side view of the upper part, which faces the airflow.

Configuration (shown in Figure 3): A square shaped Peltier module sandwiched between a square shaped aluminum flat plate, used as an active surface for the condensation, of dimension 5x5 cm^2 with thickness of 3 mm and a heat exchanger device and a temperature regulator that controls the power supply of the Peltier module. The overall arrangement was placed in a test section of a wind tunnel in which the airflow hydrodynamics, temperature and hygrometry were regulated.

Measurement: The plate temperature is constant. The condensate formed is monitored by weight of the whole system and measuring changes in weight every 30 minutes.

To complete comparison with experimental and theoretical results, the CEI-1 experiment is considered in this study [2]. This experiment was performed for a mean entrance velocity of 1.0 m/s and the mean relative humidity of 57.2 %, with the ambient temperature and pressure far from the condensing plate were 23.2°C and 926 mbar respectively, and the mean surface temperature of the plate was kept constant at 11.4°C.

The experimental average values according to Tiwari (2011) are given in Table 1.

Table 1. Input data of the experiment.

Name of Experiment	CEI-1
Atmospheric pressure, millibar	926
Amount of condensate collected, g	2.3
Data acquisition time, h:min	7:50
Ambient temperature range (mean °C)	23.2
Surface temperature (mean °C)	11.4
Relative humidity (mean %)	57.2
(Total wt/Total time), g/h	0.3142
Mass flux, kg/m²/s	$3.49 \cdot 10^{-5}$
$(m_2-m_1)/(t_2-t_1)$	0.2938
Mass flux, kg/m²/s	$3.26 \cdot 10^{-5}$
Theoretical rate of condensation, g/h	0.3175
Theoretical mass flux, kg/m²/s	$3.53 \cdot 10^{-5}$

Please note that (Total wt/Total time) is the cumulative weight of condensate divided by the total time in collecting that weight; taking the average of all data points for one experiment obtained as $(m_2-m_1)/(t_2-t_1)$, the increase in the weight of condensate in each step (every 30 min or every 0.1g increase) divided by the time taken in that step.

A 3D CFD simulation model was considered. The computational mesh with 100,000 cells was sufficient to obtain a reliable mesh for a converged solution.

Two methods for calculating experimental rate of condensation in grams per hour are shown below:

$$Mean\ rate\ of\ condensation\ (g/h) = \frac{Total\ weight\ on\ balance\ (g)}{Total\ time\ (h)} \tag{3}$$

$$Rate\ of\ condensation\ (g/h) = \frac{Increment\ in\ mass\ (m_2 - m_1)\ (g)}{Time\ this\ increment\ in\ mass\ took\ (h)} \tag{4}$$

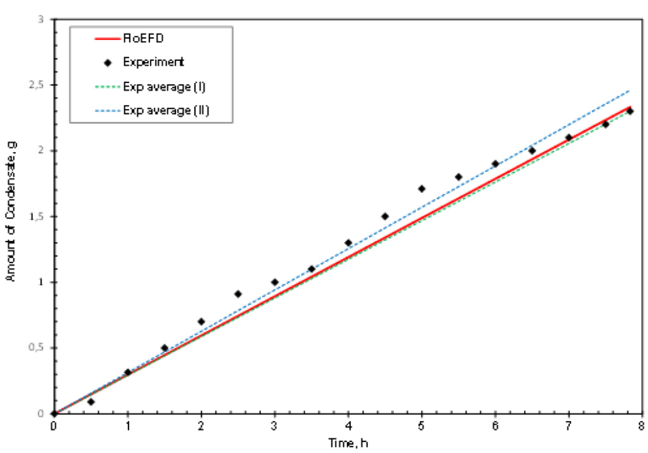

Figure 4. Amount of condensate as a function of time predicted by FloEFD and measured experimentally vs experimental measurement results

The variation of environmental parameters can affect the rate of condensation for a particular time period, which is more accurately accounted for in the second method, as the first method only produces global data. Therefore the second method was selected for the simulation study as experimental conditions did vary with time.

The amount of condensate predicted to be formed with the described method is compared against the experimental data (Tiwari, 2011), in Figure 4. A comparison of the condensation rate shows that simulation software results predict the condensation effects with good accuracy. (The relative calculation error is about 5%.)

APPLICATION TO AUTOMOTIVE HEADLIGHT

Condensation build-up inside of automotive headlights is a common occurrence which can happen for a number of reasons. While a vehicle's engine is running with the headlights on, the bulbs heat the interior space within the headlight housing. After stopping the cooler, humid air outside can migrate into the housing of the headlight. On most cars the housings are vented at the top and bottom to relieve pressure differences to prevent the bulbs and lamps from cracking and failing. If the internal surfaces of the headlight are cooler than the air inside the housing, droplets of moisture will condense inside. When the ambient or internal temperature rises, the moisture usually evaporates. Water can also leak into the headlight through cracks, broken seals or through improperly sealed housings.

This example presents the results of a numerical simulation of misting inside a headlight. The following aspects of the condensing and evaporating processes are considered in the simulation:

1. condensation of water from humid air inside a headlight;
2. accumulation and distribution of the condensate on inner surfaces of headlight;
3. freezing of the condensate;
4. melting of the frozen condensate with further evaporation by switching on bulbs.

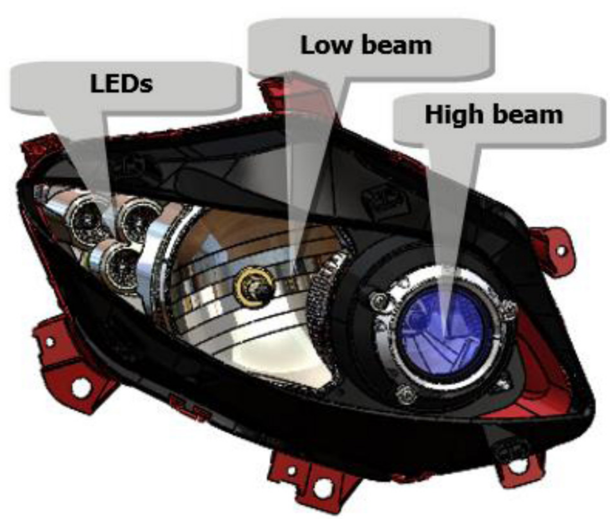

Figure 5. Headlight CAD model

In this investigation the simulation of misting inside a headlight has been applied to a geometrically complex CAD model. Film behavior has been driven by two contrary processes: initially condensation of vapor on the internal surface of the headlight's protective outer lens as the headlight cools, followed by evaporation of the condensate after switching on the filament bulbs. The headlight is equipped with high and low beam optical devices. The corresponding CAD model (Figure 5) has the same features. The low and high beam are comprised of a bulb and reflector, while the high beam additionally employs a focusing lens. Also 3 LEDs (light emitting diodes) are mounted in the corner of the headlight.

The interaction between headlight's interior volume and the environment has been modeled via a gap on the backplate. As a result a certain amount of the outside air could enter or leave the headlight during the simulation.

To promote intensive condensation two general conditions were specified:

1. The environment temperature was defined as -10 °C;
2. It was assumed that at the start of the simulation that the headlight's interior was filled with warm air at a temperature of 25 °C and a relative humidity 95% while all the solids' temperature was 20 °C.

For the simulation the properties of typical H7 car bulbs were been chosen. The filaments of the bulbs were treated as diffusive radiative sources with power 55 W and heat sources with a temperature of 2626 °C. The bulb was simulated as a glass chamber filled with krypton at 2 atm. The glass material was defined in two ways: as fully opaque in application for the bulb's tips or semitransparent with spectral dependency of absorption coefficient for the rest of the bulb's surface. Inside the bulb a tungsten spiral (main radiative source) was placed. The sticks and holders of the spiral filament were made of molybdenum. The CAD model of the H7 car bulb with the main properties is shown in Figure 6.

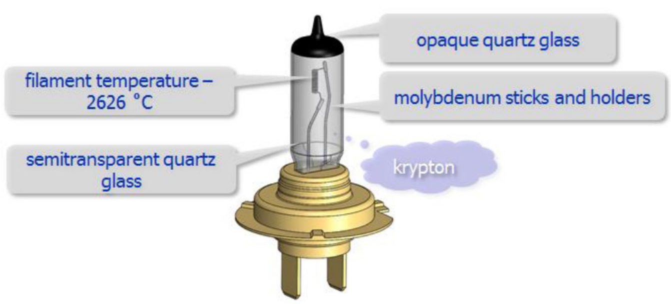

Figure 6. The CAD model of H7 bulb

LEDs were defined with a forward current equal to 400 mA. Their radiant and luminous fluxes were defined as functions of current on the basis of the Engineering Database of FloEFD (Figure 7):

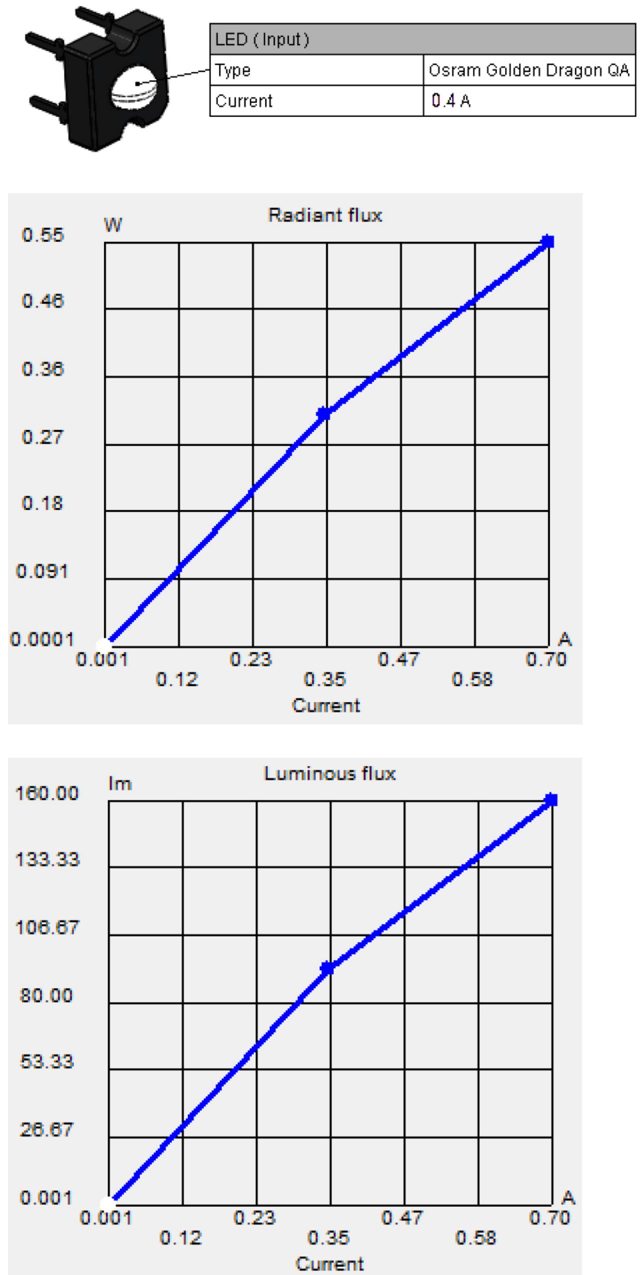

Figure 7. LEDs properties.

The operational conditions of the headlight were specified according to the previously described 2-step scenario. At the initial moment the headlight's interior volume contained hot humid air at temperature T=25 °C, pressure P=1 atm with relative humidity 95%. The initial solid temperature was 20 °C, and environment temperature was -10 °C. The task was calculated in the internal space of the headlight as a conjugate heat transfer CFD analysis including convection, conduction, and radiation. To define the external heat removal from the headlight the outer surfaces of the model were separated into 2 classifications: 1) the surfaces which would be exposed to the engine compartment or underhood region (which represented the bulk of the surfaces), and 2) the exterior surface of the outer lens, which was exposed to the outside ambient conditions. The following conditions were specified for the surfaces exposed to the engine compartment: the heat transfer coefficient was fixed with the value 2 W/(m^2·K) while the temperature of air varied as a function of time (Figure 8).

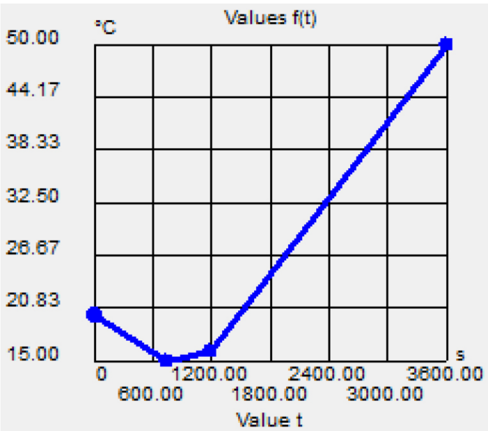

Figure 8. Dynamics of the underhood air temperature.

The surfaces of the of the front lens had a heat transfer coefficient specified as 20 W/(m^2·K) while the temperature of external ambient air was -10 °C. (Figure 9).

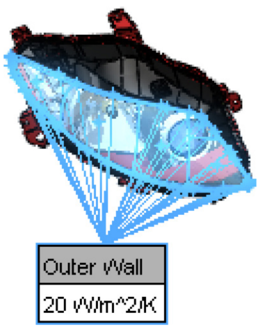

Figure 9. Front lens boundary condition

For the second stage of the scenario the LEDs and H7 car bulbs were switched on. LEDs were switched on after 12.5 min and H7 bulbs after 20 min.

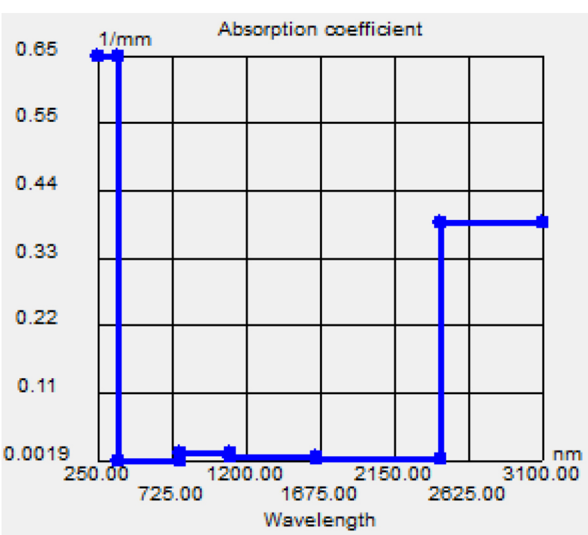

Figure 10. Absorption coefficient of the front lens as a function of wavelength.

To account for the specifics of heat transfer properly a number of solid materials were chosen. The material for the headlight's case and surrounding shell was plastic, the reflector was made of aluminum and the protective lens was quartz with refractive index 1.585. The spectral dependency of the absorption coefficient is specified in the Figure 10.

The computational mesh for the simulation contained only about 200,000 cells and can partially be seen in Figure 11:

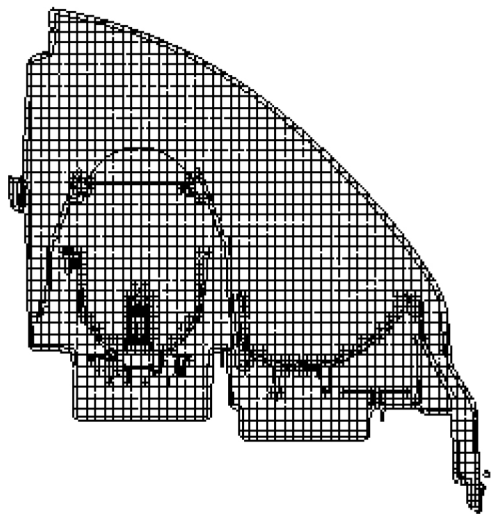

Figure 11. Computational mesh - cross-section view.

A suitable time step corresponding to the problem statement was about 10^{-2} seconds, while the simulation lifecycle lasted for 3600 seconds. The time per iteration took about 290 seconds, mostly because of the ray tracing the for the radiation processes. To reduce the computing time, a special flow field freezing technology was used. After the flow field had been converged (for about a few seconds), every 20 iteration were performed using "frozen" (fixed) values of the flow field parameters taken from the previous iteration while the time step within solids was larger and equal to 5 seconds. After the freezing period was completed, a period of relaxation was initiated. During the relaxation period a uniform time step for all the computational domain was employed (with its initial value), and the flow field was corrected. This computing strategy yielded good results while reducing the computational time of the calculations to only 1 day.

RESULTS

During the initial phase of the analysis in which the engine and lights are off the headlight assembly cools due to the low ambient temperature, which leads to condensation formation on the inside surface of the front lens. In fact, the temperature of the front lens drops below freezing generally and much of the condensation turns to ice. When the engine and lights are turned on most of the area of film melts and then evaporates.

Film Mass Dynamics

Figure 12 illustrates the overall dynamics of the film mass (a) together with temperature of the bulbs and LEDs (b) and temperature of inner lens surface (c).

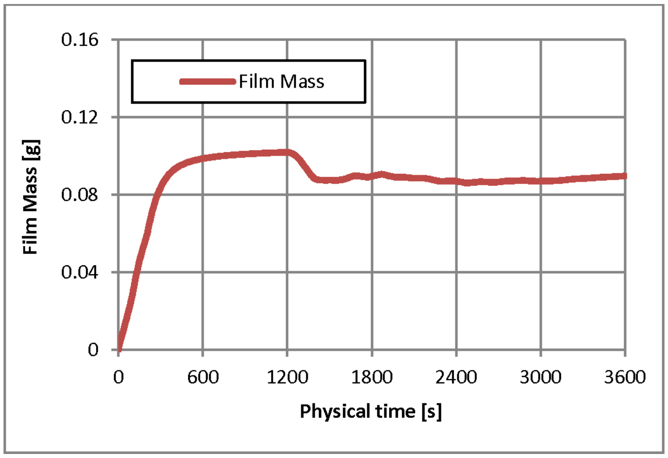

a.

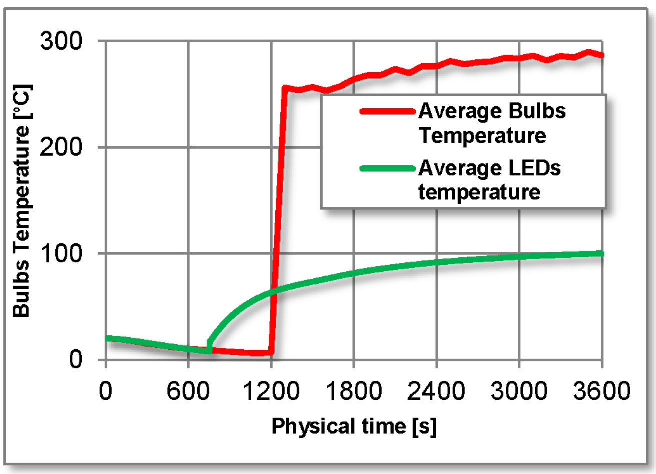

b.

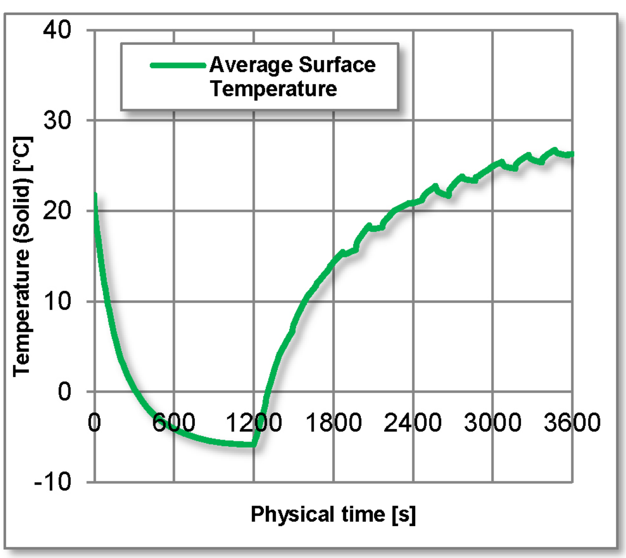

c.

Figure 12. Dynamics of film mass, temperature of bulbs and LEDs and temperature on internal surface of protective lens.

It is easy to see that prior to the bulbs being switched on that condensation occurs most intensively. This process is driven by the external cooling reducing the temperature of the inner glass surface (Figure 12, c). Switching on the LEDs after 750 seconds of physical time does not affect significantly the film evolution as their power is not enough to appreciably heat the inner glass surface. The film mass starts to decrease intensively starting at 1200 sec when the main lights and engine are turned on, which continues for about 200 seconds because of evaporation on the central part of glass. After that the condensate spreads to the cooler glass periphery. Therefore after 1400 seconds of physical time the film mass is almost constant. In spite of intensive heating of the glass and evaporation, the condensate is still being accumulated on the periphery. The temperature of the glass boundaries is kept low by the ambient conditions. At the same time as the film evaporates humidity is reintroduced into the air. This humidity in the air encounters the cooler surfaces at the periphery and again condenses, creating a situation in which evaporation is occurring at the center of the lens while simultaneously condensation is occurring along its edges.

Film Thickness Distribution

The specifics of the film evolution is represented by a series of plots of the film thickness on the internal surface of the protective glass (Figure 13). The accumulation of the condensate starts from the top of the glass (corresponding to natural convection of the humid air inside of the headlight) and continues to the boundaries (due to the ambient conditions at the periphery being cooler). Such thermal conditions cause the expected film distribution.

At the moment when the bulbs are switched on film covers most of the internal lens surface. Evaporation of the film starts from the area in front of the low beam reflector (Figure 13, 1400 s). Heat transfer from the high beam bulb is restricted by the high beam lens which absorbs a certain amount of heat that would otherwise radiate and convect directly onto the front lens. Therefore the area in front of the high beam is cleared of the film after the low beam region (Figure 13, 1800 s).

While the film is being evaporated in the main central region of the front lens, at the same time condensate is being accumulated on the glass periphery. To illustrate the different dynamics occurring regarding the film distribution 2 points were selected to quantify the film thickness - one on the central area of glass and another on the corner near the boundary (Figure 14). The central point in front of the low beam reflector contains the most heated area. The maximum film thickness was reached by 600 s and stayed constant until the bulbs were switched on. Then all the condensate at the central point was evaporated. Meanwhile, the corner point displays different behavior dynamics as the condensate is accumulated monotonically through time.

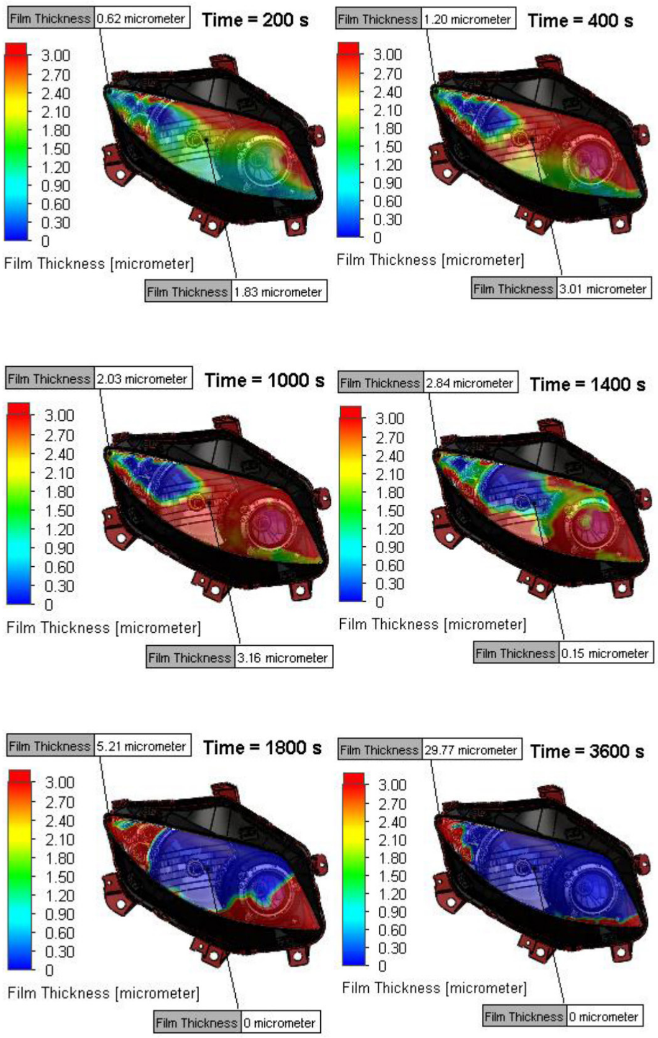

Figure 13. Surface plots of film thickness at different points of time.

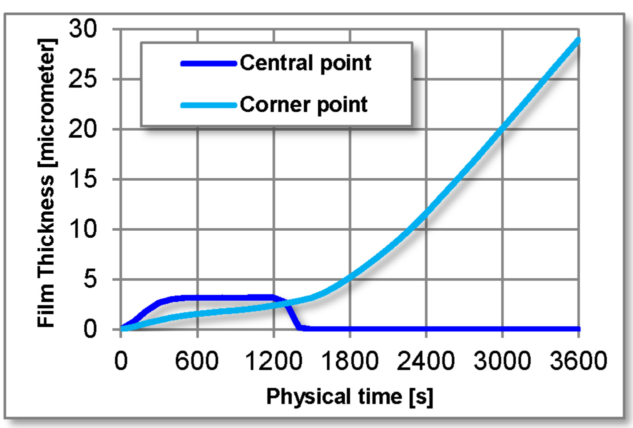

Figure 14. Film thickness dynamics

Specifics of Condensate Accumulation

During condensation the lens area in front of the LEDs and adjacent region near the low beam reflector stays almost dry. The reasons for such a distribution can be understood by analyzing the temperature distribution of the components of the headlight assembly (results shown are for 200 seconds of physical time). As we can see from Figure 15 the dry zone corresponds to hottest area of protective lens.

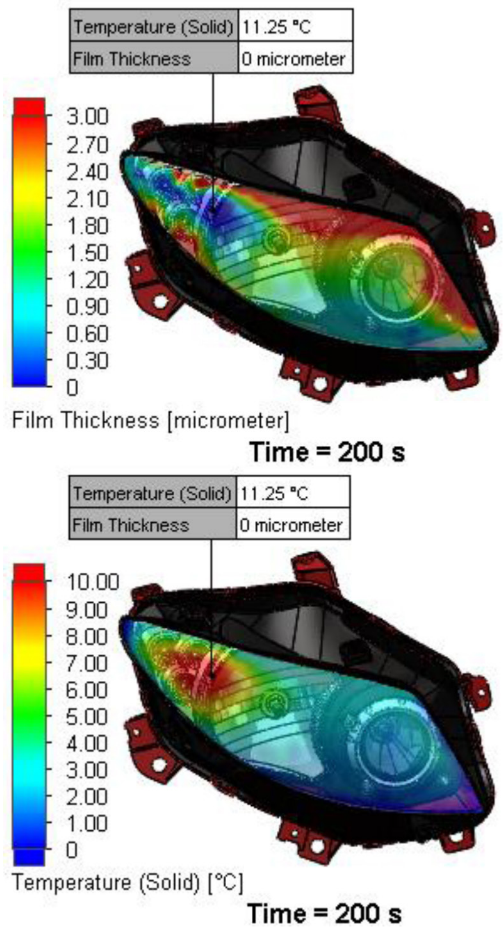

Figure 15. Distribution of film thickness and temperature on the inner surface of the protective lens.

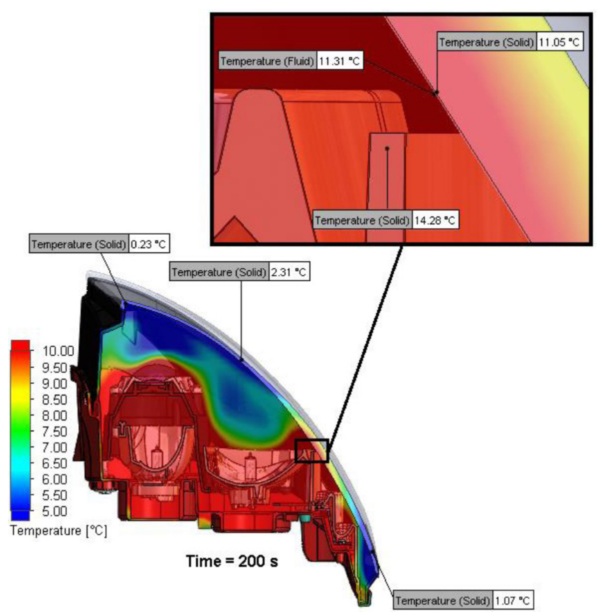

Figure 16. Distribution of temperature on the cross-section of headlight (top view).

The temperature distribution on the cross-section of the headlight (Figure 16) shows the most heated zone around the optical devices and reflectors. In this zone the air temperature has been kept close to the initial value because of low level of heat removal (construction of the corner of the model obstructs the internal convection). The lens temperature varies from about 0 °C on the periphery to 11 °C on the dry area (marked on the Figure 16 with a square). It is easy to see that the maximum solid temperature has been reached on the thickest part of the lens which is almost in contact with the hot surface of the reflector. The temperatures of the thickest part of the lens and the air circulated in this region are very close to each other and prevent condensation from forming on the lens in this area.

Film Phase

Due to the external cooling on the front lens during the first 20 minutes of physical time the film temperature decreases (Figure 17).

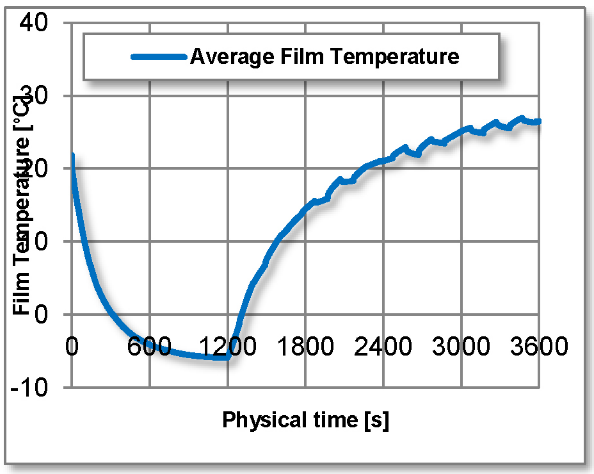

Figure 17. Dynamics of film temperature.

After 300 seconds the temperature in certain regions of the protective lens drops below 0 °C. Heat removal is enough to initiate phase transition. The dynamics of film freezing is shown in Figure 18. A value of "0" corresponds to the liquid phase (water), while a value of "1" to the solid phase (ice).

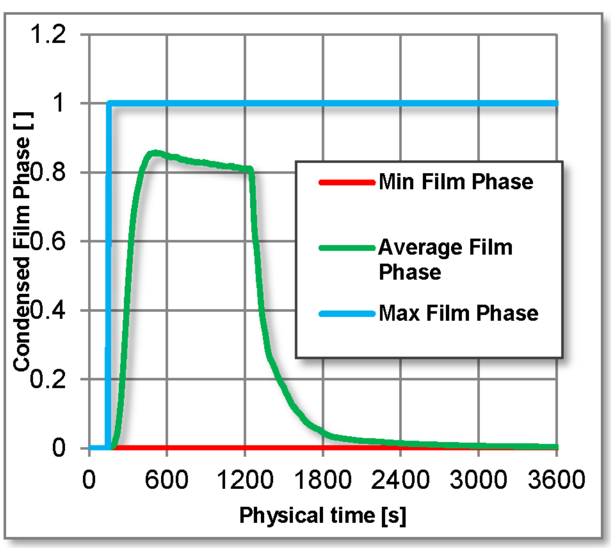

Figure 18. Film phase as a function of time.

Film phase transition starts after about 3 minutes of physical time. From that moment there are two phases of film, both ice and water. Even after melting and evaporation there are some regions covered with ice.

Distribution of the film phase as a function of time is shown in Figure 19. Due to the temperature distribution of the lens freezing starts from the bottom of the lens.

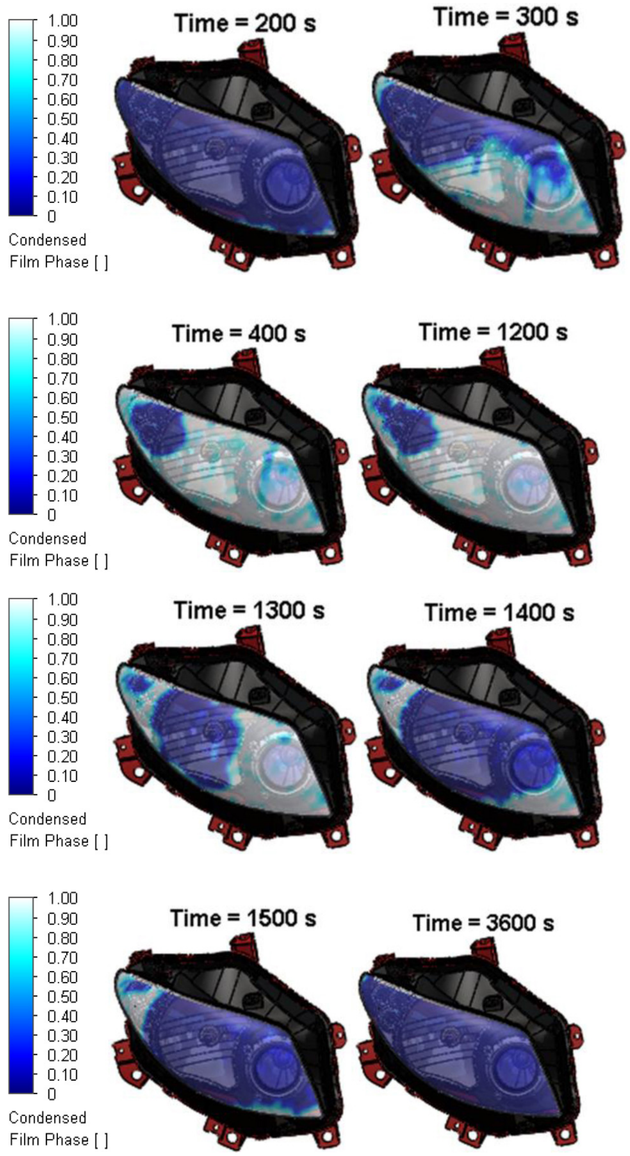

Figure 19. Condensed film phase on the internal surface of protective lens as a function of time.

Switching on the bulbs finally evaporates the condensate, but first the film needs to be heated enough to melt. About 2 minutes elapsed to raise the film temperature to 0°C. At that moment one can observe two-phase area which contains both water and ice and appears as a thawed patch (Figure 19, 1300 seconds). The remaining evaporation takes only about 5 minutes, while 40 minutes are needed to obtain a steady thermal state of the headlight. Even after most areas of the lens have dried (after 1500 seconds), small regions of the lens periphery where the temperature stays cold due to the boundary conditions and model geometry still remain covered with ice for the next 2100 seconds (as seen in the Max Film Phase shown in Figure 18).

SUMMARY/CONCLUSIONS

A specific mathematical model of surface condensation and evaporation used to perform transient simulations of liquid film formation and removal was presented. This method, implemented in a CFD Software (FloEFD), was validated with 2 experimental studies compared to simulation results. Good agreement with experimental data was obtained.

The application of the proposed mathematical model to simulate the formation of liquid film on the internal surface of a vehicle headlight's protective lens with the subsequent removal caused by switching on the lights for running operation was demonstrated as part of a comprehensive thermal CFD analysis.

REFERENCES

1. Iskra, C. R. & Simpson, C. J. (2007) Convective mass transfer coefficient for a hydrodynamically developed airflow in a short rectangular duct, Int. J. of Heat and Mass Transfer vol. 50, pp. 2376-2393.
2. Tiwari, A. (2011) Characterisation of mass transfer by condensation of humid air on a horizontal plate, PhD Thesis, Blaise Pascal University, Clermont-Ferrand, France.
3. FloEFD Technical Reference, Mentor Graphics Corp., 2015
4. Marovic Boris, Clark Mathew. Efficient and Accurate Thermal Simulation by Combining Thermal and Radiometric Characterized LEDs with Computational Fluid Dynamics. Mentor Graphics (Deutschland) GmbH.

CONTACT INFORMATION

Christopher Watson
Mentor Graphics Corp
chris_watson@mentor.com